AL-Bahir
Journal for Engineering and Pure Sciences
BJEPS

Volume 2 | Issue 2 Article 7

Green synthesis of Nickel Oxide Nanoparticles using Syzygium Aromatic Extract: Characterization and Biological Applications

Shaimaa M. Jassim
Directorate general of education in Diyala, Diyala, Iraq

Mohammed A. Abd
Directorate general of education in Diyala, Diyala, Iraq

Israa A. Hammed
Directorate general of education in Diyala, Diyala, Iraq

ORIGINAL STUDY

Green Synthesis of Nickel Oxide Nanoparticles Using Syzygium Aromatic Extract: Characterization and Biological Applications

Shaimaa M. Jassim*, Mohammed A. Abed, Israa A. Hameed

Diyala Directorate General of Education, Diyala, Iraq

Abstract

In this study, nickel oxide (NiO) nanoparticles were successfully synthesized by *Syzygium aromaticum* (clove) extract via a green synthesis method and evaluated their antibacterial properties. The bio-molecules inside the extract play an important role in converting nickel nitrate salt into nickel oxide nanoparticles. The prepared nickel oxide nanoparticles were characterized via different techniques such as X-ray Diffraction, fourier transform infrared spectroscopy, field emission-scanning electron microscopy and ultraviolet−visible spectrophotometer. From X-ray diffraction results, the crystallite size of NiO NPs was estimated to be (39.7 nm). The fourier transform infrared spectroscopy exhibits intense two peaks at 594 cm^{-1} and 469 cm^{-1} which indicates the formation of NiO NPs. In addition, the energy band-gap calculated by Tauc's formula was ~2.89 eV. Finally, The antibacterial activity study results detected that NiO NPs have the highest activity against *Staphylococcus aureus* when compared to *Escherichia coli*. Thus, the present study exhibits good antibacterial activity, which may be explored in future clinical treatments.

Keywords: Syzygium aromaticum extract, Green synthesis, Nickel oxide nanoparticles, X-ray diffraction, Gram positive, Antibacterial applications

1. Introduction

Nanotechnology is one of the most significant technologies used in broad research fields via investigators across the world recently due to its unique characteristics [1]. Nanoscale materials depicted beneficial chemical and physical properties being dissimilar to the bulk materials properties [2]. The nanoparticles of metal oxide are of highly attention due to their distinctive and unique properties, such as optical, electronic, magnetic and mechanical properties [3,4].

The nanoparticles of NiO have taken much attention in the latest studies, due to the high chemical stability; splendid conductance features; as well as good optical, electrical, and magnetic properties [5]. Nickel oxide nanoparticles (NiO NPs) are a p-type semiconductor metal oxide with a broad band-gap range (3.6−4.0 eV) [6,7].

NiO NPs have a wide range of uses in the fields of catalysts, electrodes of fuel cell, solar energy absorption, magnetic recording media, magnetic fluids, permanent magnets, and antimicrobial action [8,9]. NiO nanoparticles were discovered to be toxic to bacteria due to their ability to induce oxidative stress and release nickel ions (Ni^{2+}) within the cell, this is attributed to their unique properties [3].

Numerous physical and chemical approaches are used for NiO NPs synthesis, such as sol−gel method, electro-deposition, laser ablation, electrospray synthesis and galvanostatic anodization. Nevertheless, such fabricating approaches accompanied many disadvantages, like toxicity, low productivity and not eco-friendly [10, 11]. To overcome these problems, non-hazardous and environmental friendly biological methods were proposed [12]. Recently, the nanoparticles of metal oxide have been fabricated employing the extracts of plants and

Received 25 February 2023; revised 18 March 2023; accepted 3 April 2023.
Available online 1 May 2023

* Corresponding author.
E-mail address: shema119988@yahoo.com (S.M. Jassim).

https://doi.org/10.55810/2313-0083.1024

microorganisms in a fast, active, economic, and simple method [13]. These extracts were utilized as reducing and capping agents into the green chemistry method [14]. *Syzygium aromaticum*, normally recognized as clove, has been utilized in the current study for preparing nickel oxide nanoparticles (NiO NPs). The clove is a flower bud from a tree that belongs to the family of Myrtaceae. It's well-known for its typical aroma owing to the eugenol existence, and it's also rich in non-volatile antioxidants that belong to the polyphenols group, including aromatic hydroxy acids, flavonoids, hydrolysable tannins, and their glycosylated derivatives. The cloves manifest antiseptic, antiviral anti-bacterial, and antifungal properties [15]. Vijaya et al. [16] studied the anti-bacterial activity of NiO NPs against more types of pathogenic bacteria. Muhammad et al. [17] proved the sensitivity of bacteria against different strains *(Staph. aureus, E.coli)* of bacterial using NiO NPs. V. Helan et al. [18] studied the cytotoxic activity of NiO NPs against bacterial pathogens such as *Staphylococcus aureus* and *Escherichia coli* by agar diffusion assay. Ramasami et al. [19] examined antimicrobial activity against one fungal (*Candida albicans*) and two bacterial (*Bacillus cereus* and Klebsiella aerogenes) strains treated with NiO NPs. Stapylococcus aureus and *E. coli*, two prevalent food-borne harmful bacteria, were used by Talebian et al. [20] to assess the antibacterial efficacy of NiO NPs. In the present research, to the best of our knowledge, the green synthesis of NiO NPs with *S. aromaticum* (Clove) flowers has not yet been reported. Antioxidant biological moieties present in the clove extract enabled it to act as a reducing agent as well as a stabilizing agent for NiO NPs. NPs samples were characterized using various techniques, such as XRD, UV−Vis, FTIR, and FESEM. Finally, the prepared NiO NPs were tested for biological effects.

2. Materials and methods

2.1. Used materials

Nickel (II) nitrate hexahydrate ($Ni(NO_3)_2.6H_2O$, Sigma−Aldrich), *S. aromaticum* (Clove) flower buds, was purchased from the local market (Iraq, Diyala), and the distilled water was used as a solvent.

2.2. Synthesis of clove extract

Cloves dried flower buds were washed by distilled water for removing the impurities. Then, these cleaned buds were ground into a pestle and mortar to a fine powder. After that, twenty grams of flower powder were added to (100 ml) of distilled water and left to be continuously stirred for 30 min at 70 °C. The obtained extract was first exhaustively filtered employing Whatmann No. 1 filter paper and then cooled to room temperature.

2.3. Synthesis of NiO NPs

Nickel nitrate ($Ni(NO_3)_2$) was utilized as a precursor, and 100 ml of the clove extract filtrate were added dropwise to a (100 ml) aqueous $Ni(NO_3)_2$ solution using a magnetic stirrer at (70 °C) for (30 min). Through stirring, the solution's color suddenly changed from a dark green to a light green color, and this is attributed to NiO nanoparticles formation. Then, 50 ml of the mixed solution were placed into a ceramic crucible and annealed at 600 °C for 2 h. Finally, the fine powder of NiO NPs was obtained and used for further studies.

2.4. Characterization

Different methods were employed to characterize the NiO NPs. The crystalline nature, phase purity, and crystallite size of the synthesized NiO NPs were determined by using X-ray diffractometer instrument (XRD, Shimadzu 6000, Japan) utilizing the radiation of CuKα (λ = 1.5406 Å). And, the functional groups of NiO NPs were identified by fourier transform infrared (FTIR) spectrophotometer (Shimadzu 8000). To investigate the morphology of the produced nanomaterial surface, a field emission-scanning electron microscope (FE-SEM), type MIRA3 TESCAN, was utilized. The optical absorbance for NPs was carried out via (UV−Vis−NIR) spectrophotometer (Shimadzu, UV-1800) at room temperature.

3. Antibacterial activity

The Agar diffusion method was used to study the anti-bacterial action of the synthesized nickel oxide nanoparticles (NiO NPs). This method was employed against gram-negative bacteria and gram-positive bacteria (*Escherichia coli* (*E. coli*) and *Staphylococcus aureus* (*S. aureus*)), respectively. Different concentrations (25, 50, 75 and 100 μg/ml) of the NiO NPs solution were spread into each dish. All the dishes were brood at 37 °C for 24 h, and the respective inhibition regions were then measured. After 24 h, by measuring the diameter of the inhibition region surrounding each hole, the effectiveness of each concentration was calculated.

4. Results and discussion

4.1. XRD analysis

The XRD pattern was utilized for investigating the structural information as well as the crystallinity of NiO NPs made with clove plant extract. Also, the XRD pattern of the NiO powder derived from the breakdown of the annealed precursor at a temperature of 600 °C is evinced in Fig. 1. There are five powerful Bragg's peaks with their maxima centered into the mid at (2θ ~ 37.28°, 43.31°, 62.90°, 75.46°, and 79.40°), respectively. The detected peaks of diffraction matching to the planes of (1 1 1), (2 0 0), (2 2 0), (3 1 1), and (2 2 2) are properly attributed to the cubic structure of NiO, which is corresponded to the international center of diffraction data (ICDD) card number (047-1049). These results are in good agreement to a literature reported by Mayedwa et al. [1]. The comparatively elevated intensities of the peak imply that the nano powders of nickel oxide (NiO) have a high crystallinity. Table 1 displays the structural parameters of synthesized NiO nanoparticles. The crystallite size (D) is estimated using the specifications of the peak corresponding to the (2 0 0) plane by Scherrer's equation [21].

$$D = \frac{K\lambda}{\beta \cos\theta} \quad (1)$$

where:

K: Constant = 0.9

λ: The wavelength (0.15406 nm) of X-ray

β: The Full Width at Half Maximum (FWHM), in radian

θ: The angle of Bragg, in degree.

And, the crystalline size of prepared NiO nanoparticles was computed using Scherer's equation and was found to be 39.7 nm.

Table 1. Structural parameters of NiO NPs.

List	2θ (deg.)	(hkl)	FWHM (deg.)	d-space (Å)
1	37.32	(1 1 1)	0.272	2.408
2	43.35	(2 0 0)	0.271	2.085
3	62.92	(2 2 0)	0.322	1.476
4	75.46	(3 1 1)	0.335	1.259
5	79.43	(2 2 2)	0.324	1.205

4.2. Fourier transfer infrared (FTIR) analysis

In the FTIR spectroscopy of NiO NPs annealed at 600 °C, Fig. 2 elucidates a wide band of absorption at 3488 cm^{-1} that can be attributed to the O–H stretching vibration. There was also a (1620 cm^{-1}) absorption spectrum observed, which was associated with the bending vibrations of water molecules [22]. The 2353 cm^{-1} spectrum is hypothesized to be caused by CO_2 molecules in the air [23]. The 1386 cm^{-1} spectrum is caused by the stretching of NO_3 at 1118 cm^{-1} [5], and the C–O bands due to the (Co) adsorption can be seen [24]. The vibration of the Ni–O bands caused a strong band at 594 cm^{-1} and the other at 469 cm^{-1} [22]. Table 2 exhibits the values of the possible assignment of the absorption bands of NiO NPs synthesized using a simple chemical method.

4.3. Field emission-scanning electron microscope (FE-SEM) analysis

The FE-SEM micrographs of synthesized NiO nanoparticles are displayed in Fig. 3. From this figure, it was noticed that these particles are merged together and embedded in the nearby particles (agglomerated particles). And, the agglomerated nanoparticles of NiO exhibited an amorphous form. Also, the NiO nanoparticles agglomeration portrayed via FE-SEM is owing to the forces of Van der

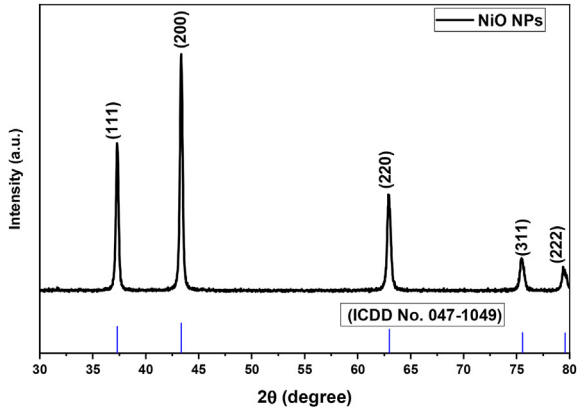

Fig. 1. XRD pattern of NiO nanoparticles.

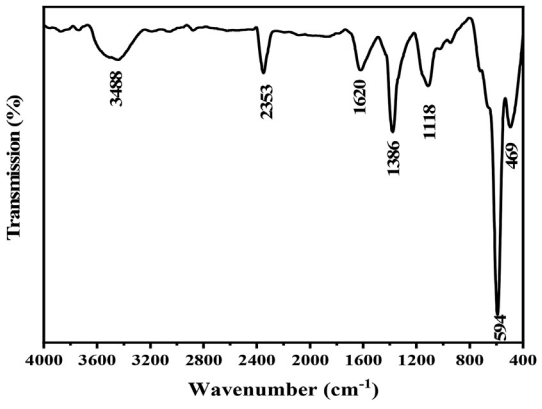

Fig. 2. FTIR spectroscopy of NiO NPs.

Table 2. FTIR peaks assignments of green synthesized NiO NPs.

SI. No.	NiO NPs	Assignment
1	3488	O–H stretching
2	2353	O–C–O bending
3	1620	H–O–H bending
4	1386	N–O stretching
5	1118	C–O bending
6	594	Ni–O stretching
7	469	Ni–O stretching

Waals that draw these particles together. As well, this highly takes place into the nanoparticles having smaller dimensions. The agglomeration can be attributed to that the nanoparticles of NiO have a high surface energy and a high surface tension of the ultra-fine nanoparticles. Furthermore, the secondary metabolites obtained in the extract of plant, which decreases the nitrate precursor into the nanoparticles, can also influence the fabricated NiO NPs size [25].

4.4. UV–vis analysis

The optical properties and electronic structure of the optical energy gap of prepared material were investigated using UV–Vis–NIR spectroscopy. As shown in Fig. 4, the absorption spectrum of the manufactured nickel oxide sample occurs in the ultraviolet and near-visible regions of the electronic transitions associated with the sample. The absorption spectrum diminishes with increasing the wavelength due to the intensity of incident electrons and their ability to irritate the electrons from the conduction band and band valence.

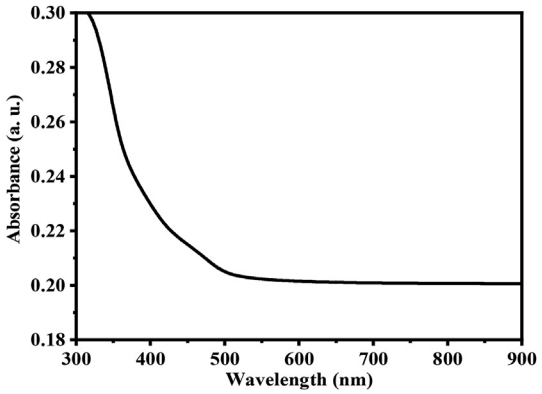

Fig. 4. UV–Vis absorption spectrum of NiO NPs.

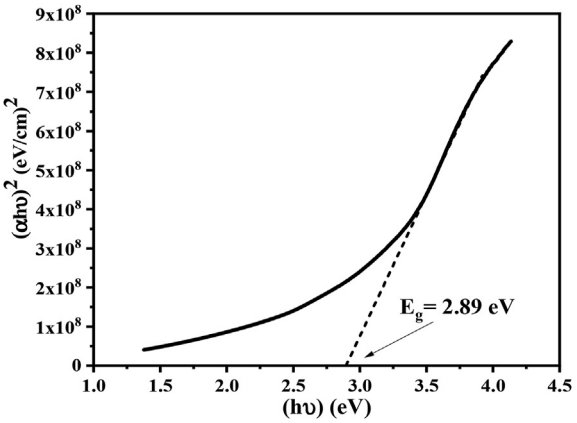

Fig. 5. Tauc's plot of NiO NPs.

Using the Tauc's formula, the optical band-gap (E_g) of the synthesized NiO NPs was calculated [26]:

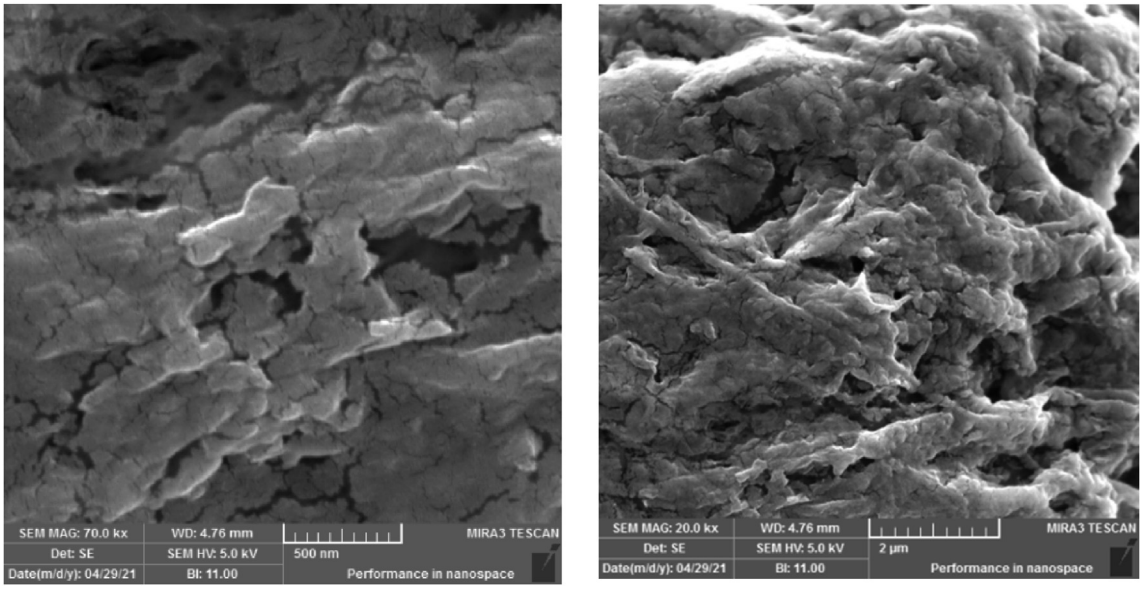

Fig. 3. FE-SEM images of NiO NPs.

Table 3. Inhibition zones (mm) of NiO nanoparticles produced.

Concentrations (µl)	Zone of inhibition (mm)	
	Gram (−ve) *E. coli*	Gram (+ve) *S. aureus*
100	26	33
75	24	31
50	21	25
25	17	22

$$(\alpha h\upsilon) = A\left(h\upsilon - E_g\right)^n \quad (2)$$

Where, (A) is constant, (α) is the optical absorption coefficient, ($h\upsilon$) stands for the energy of photon, and (n) is an empirical quantity that describes the electronic transition type which is equal to ½ for direct allowed transition. In this study, a straight line was generated by sketching a plot between $(\alpha\, h\upsilon)^2$ and ($h\upsilon$). Then, the direct band-gap could be estimated by extrapolating this straight line to $(\alpha\ h\upsilon)^2 = 0$, as illustrated in Fig. 5. The estimated value of E_g was found to be (2.89 eV), which is lower than the value published in the literature [5,22].

4.5. Antimicrobial activity of NiO NPs

The nanoparticle concentration was adjusted between 25 and 100 µl. The antibacterial activity was observed in the NiO nanoparticles that were produced. Table 3 shows the diameter of the strain in millimeters. It is commonly known that when the anti-bacterial inhibition region diameter is greater than 6 mm, the sample enhances the antibacterial activity. And, the sample exhibits inferior anti-bacterial action when the diameter of the anti-bacterial inhibition region is ≤ 6 mm [27]. Also, the anti-bacterial inhibition region for the Gram-positive and Gram-negative bacteria studied is substantially

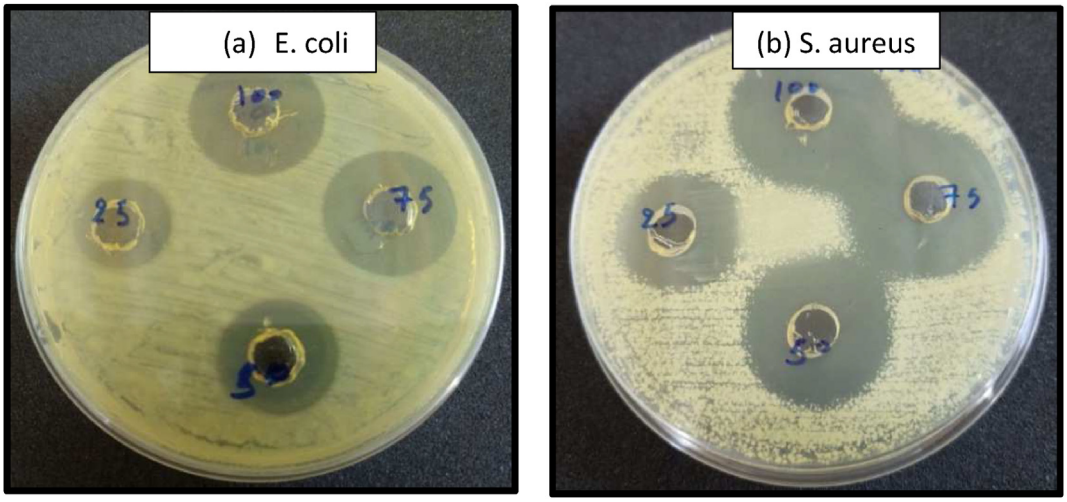

Fig. 6. The antimicrobial effect in Nickel Oxide NPs (a) E. coli and (b) S. aureus.

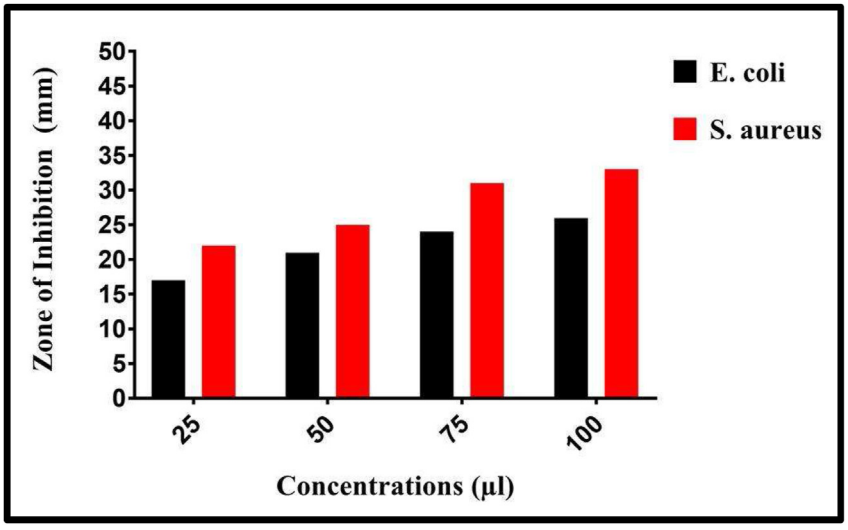

Fig. 7. NiO NPs' zone of inhibition for E. coli and S. aureus.

larger than 6 mm for the nanoparticles, as depicted in Table 3 and Fig. 6. The antibacterial activity of NiO nanoparticles is much stronger against S. aurous compared with *E. coli*, and this result agrees well with reference [28]. The anti-bacterial property of NPs is usually determined by their smaller crystallite size and higher surface area. Negatively charged metal ions and positively charged cell membranes tempted each other, and the metal ions diffused into them. Proteins diffuse into the bacterial cell membrane, and the nanoparticle-induced inactivation of proteins reduces the cell permeability [29]. The existence of more ROS, which is mainly due to the smaller particle size and less agglomerated particles, and the diffusion capacity of reactant molecules determine the anti-bacterial efficacy of NiO NPs [30]. From Fig. 7, the inhibition zone is manifested via the nanoparticles of NiO versus the *E. coli* and *S. aureus*, and it's obvious from the results that the Gram-positive bacteria (*S. aureus*) were highly vulnerable to the nanoparticles of NiO in comparison to the Gram-negative bacteria (*E. coli*).

5. Conclusion

In summary, NiO nanoparticles have been successfully prepared by a novel, simple, efficient, and eco-friendly chemical method by employing clove plant extract as a reducing and stabilizing agent. The characterization of the synthesized sample confirmed the successful formation of NiO nanostructures. The XRD analysis result elucidated that the synthesized NiO NPs have a cubic phase with a crystallite size of about 39.7 nm. In the FTIR analysis, the achieved typical bands confirmed the results of the XRD, submitting the typical NiO binding bands of the cubic phase. In addition, the FE-SEM images clearly evinced that the produced nanoparticles had spherical-like shapes. Moreover, the UV−Vis−NIR spectra analysis revealed the strong absorbance in the visible range, and the optical band gaps of (2.89 eV) were illustrated from the spectra as well. Finally, antibacterial activity was done through the disc diffusion method using gram-negative (*S. aureus*) and gram-positive (*E. coli*) bacterial strains. The anti-bacterial study results exhibited that the NiO nanoparticles have a significant impact on the Gram-positive (*S. aureus*) more than the Gram-negative (*E. coli*).

Disclosure of funding

This research did not receive any specific grant from funding agencies in the public, commercial, or not-for-profit sectors.

Conflict of interest

None declared.

References

[1] Mayedwa N, Mongwaketsi N, Khamlich S, Kaviyarasu K, Matinise N, Maaza M. Green synthesis of nickel oxide, palladium and palladium oxide synthesized via Aspalathus linearis natural extracts: physical properties & mechanism of formation. Appl Surf Sci 2018;446:266−72.
[2] Imran Din M, Rani A. Recent advances in the synthesis and stabilization of nickel and nickel oxide nanoparticles: a green adeptness. Int J Anal Chem 2016;2016.
[3] Ezhilarasi AA, Vijaya JJ, Kaviyarasu K, Maaza M, Ayeshamariam A, Kennedy LJ. Green synthesis of NiO nanoparticles using Moringa oleifera extract and their biomedical applications: cytotoxicity effect of nanoparticles against HT-29 cancer cells. J Photochem Photobiol B Biol 2016;164:352−60.
[4] Fomekong RL, et al. Effective reduction in the nanoparticle sizes of NiO obtained via the pyrolysis of nickel malonate precursor modified using oleylamine surfactant. J Solid State Chem 2016;241:137−42.
[5] Anand GT, Nithiyavathi R, Ramesh R, Sundaram SJ, Kaviyarasu K. Structural and optical properties of nickel oxide nanoparticles: investigation of antimicrobial applications. Surface Interfac 2020;18:100460.
[6] Vasudeo K, Pramod K. Biosynthesis of nickel nanoparticles using leaf extract of coriander. Biotechnol Ind J 2016;12(11):1−6.
[7] Ezhilarasi AA, Vijaya JJ, Kaviyarasu K, Kennedy LJ, Ramalingam RJ, Al-Lohedan HA. Green synthesis of NiO nanoparticles using Aegle marmelos leaf extract for the evaluation of in-vitro cytotoxicity, antibacterial and photocatalytic properties. J Photochem Photobiol B Biol 2018;180:39−50.
[8] Sasi B, Gopchandran KG, Manoj PK, Koshy P, Rao PP, Vaidyan VK. Preparation of transparent and semiconducting NiO films. Vacuum 2002;68(2):149−54.
[9] Hussein BY, Mohammed AM. Biosynthesis and characterization of nickel oxide nanoparticles by using aqueous grape extract and evaluation of their biological applications. Results Chem 2021;3:100142.
[10] Hernández-Morales L, et al. Study of the green synthesis of silver nanoparticles using a natural extract of dark or white Salvia hispanica L. seeds and their antibacterial application. Appl Surf Sci 2019;489:952−61.
[11] Khalil AT, et al. Sageretia thea (Osbeck.) modulated biosynthesis of NiO nanoparticles and their in vitro pharmacognostic, antioxidant and cytotoxic potential. Artif Cells Nanomed Biotechnol 2018;46(4):838−52.
[12] Thema FT, Beukes P, Gurib-Fakim A, Maaza M. Green synthesis of Monteponite CdO nanoparticles by Agathosma betulina natural extract. J Alloys Compd 2015;646:1043−8.
[13] Lee H-J, Lee G, Jang NR, Yun JH, Song JY, Kim BS. Biological synthesis of copper nanoparticles using plant extract. Nanotechnology 2011;1(1):371−4.
[14] Kar A, Ray AK. Synthesis of nano-spherical nickel by templating hibiscus flower petals. J Nanosci Nanotechnol 2014;2(2):17−20.
[15] Ajitha B, Reddy YAK, Lee Y, Kim MJ, Ahn CW. Biomimetic synthesis of silver nanoparticles using Syzygium aromaticum (clove) extract: catalytic and antimicrobial effects. Appl Organomet Chem 2019;33(5):e4867.
[16] Vijaya Kumar P, Jafar Ahamed A, Karthikeyan M. Synthesis and characterization of NiO nanoparticles by chemical as well as green routes and their comparisons with respect to cytotoxic effect and toxicity studies in microbial and MCF-7 cancer cell models. SN Appl Sci 2019;1:1−15.
[17] Nawaz M, et al. Synthesis, characterization and antibacterial activity of NiO NPs against pathogen. Inorg Chem Commun 2020;122:108300.

[18] Helan V, et al. Neem leaves mediated preparation of NiO nanoparticles and its magnetization, coercivity and antibacterial analysis. Results Phys 2016;6:712–8.
[19] Ramasami AK, V Reddy M, Balakrishna GR. Combustion synthesis and characterization of NiO nanoparticles. Mater Sci Semicond Process 2015;40:194–202.
[20] Talebian N, Doudi M, Kheiri M. The anti-adherence and bactericidal activity of sol–gel derived nickel oxide nanostructure films: solvent effect. J Sol Gel Sci Technol 2014; 69(1):172–82.
[21] Jassim SM, Bakr NA, Mustafa FI. Synthesis and characterization of MAPbI 3 thin film and its application in C-Si/perovskite tandem solar cell. J Mater Sci Mater Electron 2020; 31:16199–207.
[22] Kayani ZN, Butt MZ, Riaz S, Naseem S. Synthesis of NiO nanoparticles by sol-gel technique. Mater Sci 2018;36(4):547–52.
[23] Jayakumar G, Irudayaraj AA, Raj AD. Photocatalytic degradation of methylene blue by nickel oxide nanoparticles. Mater Today Proc 2017;4(11):11690–5.
[24] Sharma AK, Desnavi S, Dixit C, Varshney U, Sharma A. Extraction of nickel nanoparticles from electroplating waste and their application in production of bio-diesel from biowaste. Int J Chem Eng Appl 2015;6(3):156.
[25] Lefojane R, et al. Green synthesis of nickel oxide (NiO) nanoparticles using Spirostachys africana bark extract. Asian J Sci Res 2020;13:284e91.
[26] Abed MA, Bakr NA, Mohammed SB. Synthesis and characterization of chemically sprayed Cu2FeSnS4 (CFTS) thin films: the effect of substrate temperature. Mater Sci Forum 2021;1039:434–41.
[27] Karthik K, Dhanuskodi S, Gobinath C, Prabukumar S, Sivaramakrishnan S. Multifunctional properties of microwave assisted CdO–NiO–ZnO mixed metal oxide nanocomposite: enhanced photocatalytic and antibacterial activities. J Mater Sci Mater Electron 2018;29:5459–71.
[28] Bhat SA, et al. Photocatalytic degradation of carcinogenic Congo red dye in aqueous solution, antioxidant activity and bactericidal effect of NiO nanoparticles. J Iran Chem Soc 2020;17:215–27.
[29] Kannan K, Radhika D, Nikolova MP, Sadasivuni KK, Mahdizadeh H, Verma U. Structural studies of bio-mediated NiO nanoparticles for photocatalytic and antibacterial activities. Inorg Chem Commun 2020;113:107755.
[30] Umaralikhan L, Jaffar MJM. Antibacterial and anticancer properties of NiO nanoparticles by co-precipitation method. J Adv Appl Sci Res 2016;1(4):24–35.